

# Structure of Pt(111)/Ionomer Membrane Interface and Its Bias-Induced Change in Membrane Electrode Assembly

Takuya Masuda,<sup>†,‡</sup> Hitoshi Fukumitsu,<sup>†,‡</sup> Toshihiro Kondo,<sup>§</sup> Hideo Naohara,<sup>‡</sup> Kazuhisa Tamura,<sup>||</sup> Osami Sakata,<sup>⊥</sup> and Kohei Uosaki<sup>\*,†,‡,∇</sup>

<sup>†</sup>Global Research Center for Environment and Energy Based on Nanomaterials Science (GREEN), National Institute for Materials Science (NIMS), Tsukuba 305-0044, Japan

<sup>‡</sup>Division of Chemistry, Graduate School of Science, Hokkaido University, Sapporo 060-0810, Japan

<sup>§</sup>Graduate School of Humanities and Sciences, Ochanomizu University, Ohtsuka, Bunkyo-ku, Tokyo 112-8610, Japan

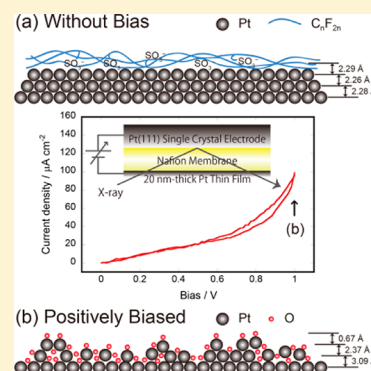
<sup>||</sup>Quantum Beam Science Directorate, Japan Atomic Energy Agency (JAEA), Hyogo 679-5148, Japan

<sup>⊥</sup>Japan Synchrotron Radiation Research Institute/SPring-8, Kouto, Sayo-cho, Sayo-gun, Hyogo 679-5198, Japan

<sup>∇</sup>International Center for Materials Nanoarchitectonics (MANA), National Institute for Materials Science (NIMS), Tsukuba 305-0044, Japan

## Supporting Information

**ABSTRACT:** The structure of the perfluorosulfonated ionomer (PFSI)/Pt(111) interface in a membrane electrode assembly (MEA)-like configuration of a polymer electrolyte membrane (PEM) fuel cell, that is, a vacuum evaporated Pt layer/PEM(Nafion membrane)/PFSI(adhesion Nafion layer)/Pt(111) single crystal, and its bias-induced change were investigated by surface X-ray scattering measurement at an atomic level. Crystal truncation rod measurement shows that PFSI adsorbed on the Pt(111)-(1 × 1) surface without bias. When the Pt(111) electrode was positively biased to form Pt oxide, the PFSI layer was detached from the Pt surface and oxygen atoms penetrated into the Pt lattice.



## INTRODUCTION

The polymer electrolyte membrane (PEM) fuel cell is one of the most promising candidates for a new-generation energy conversion device because of its high theoretical efficiency for the conversion of chemical energy to electrical energy.<sup>1–6</sup> The PEM fuel cell is composed of a stack of a membrane electrode assembly (MEA), which is constructed of binding carbon-supported platinum catalyst layers with perfluorosulfonated ionomer (PFSI) on both sides of the PEM. Platinum is an excellent electrocatalyst for fuel cell reactions, such as hydrogen oxidation<sup>7,8</sup> and oxygen reduction.<sup>9,10</sup> However, since Pt is a very expensive element of limited resource, reduction of usage and degradation control of Pt are the major issues of PEM fuel cells toward their widespread use. The degradation process of Pt catalysts within fuel cells has been extensively studied, and dissolution/agglomeration of Pt catalysts at the ionomer/Pt interface is currently considered to be one of the primary origins for the degradation.<sup>3</sup> It was proposed that dissolution of Pt was affected not only by the potential and size of particles but also by formation of Pt oxide because the oxide layer can protect the platinum from dissolution (see ref 3 and references therein). The understanding of the oxide formation process at an atomic level is, however, not clear, and utilizing a well-

defined Pt single crystalline electrode is essential to clarify the origin of the degradation and to design a long-lived catalyst.

Although scanning probe microscopy is very powerful to probe the surface structure and its change with an atomic resolution in electrochemical conditions,<sup>11–16</sup> it cannot observe the surface structure covered by an overlayer, such as an ionomer membrane. In this respect, surface X-ray scattering (SXS) is the best method to investigate the structure of such a buried interface in an atomic resolution because X-rays can penetrate the PEM and/or ionomer overlayer without significant scattering and absorption.<sup>17–23</sup> Here, we utilized the SXS technique to determine the structure of the PFSI/Pt(111) interface in a Pt/PEM/PFSI/Pt(111) sandwich configuration and its positive bias-induced change at an atomic resolution.

## EXPERIMENTAL SECTION

In this study, Nafion, which has a polytetrafluoroethylene backbone with perfluorinated ether side chains terminated by

Received: March 5, 2013

Revised: April 26, 2013

Published: May 20, 2013



sulfonic acid groups, as shown in Figure 1, was used both as a PEM and ionomer. One side of a Nafion membrane (NRE-

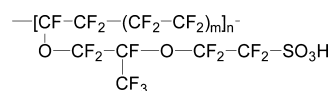


**Figure 1.** Chemical formula of Nafion.

211CS; thickness: 25.4  $\mu\text{m}$ ; DuPont Fuel Cells) was coated with a sputter-deposited 20 nm thick Pt thin film. A Pt(111) single-crystal disk (Surface Preparation Laboratory; diameter: 10 mm; thickness: 5 mm) was annealed at 1600  $^{\circ}\text{C}$  for 12 h under an argon/hydrogen flow by using an induction heater (HOTSHOT-2 kW, Ameritherm).<sup>24</sup> Additional annealing of the Pt(111) disk electrode was carried out at 1600  $^{\circ}\text{C}$  for 2 h under an argon/hydrogen flow. After cooling under the argon/hydrogen flow for 5 min, the surface was quenched by pure water saturated with argon/hydrogen, and then dipped into a Nafion aqueous dispersion (DE1020 CS; polymer content: 10–12 wt %; DuPont) to form an adhesion PFSI layer. The surface coated with a droplet of Nafion dispersion was then attached to the other side of the Pt thin film-coated Nafion membrane, so that a Pt thin film/PEM(Nafion membrane)/PFSI(adhesion Nafion layer)/Pt(111) structure, which is an approximation of the MEA configuration, was formed, as shown in the inset of Figure 2.

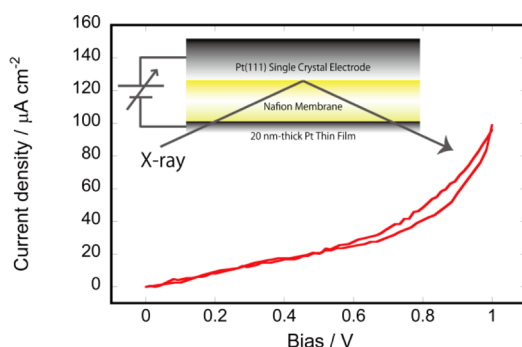


**Figure 2.**  $I$ – $V$  curve of the Pt thin film/PEM/PFSI/Pt(111) electrode measured in air saturated with water vapor.

A homemade spectroelectrochemical cell was used for in situ SXS measurement. The spectroelectrochemical cell was set on a four-circle diffractometer (Kohzu) installed in an undulator-magnet beamline BL13XU at SPring-8. X-ray radiation was monochromated by a Si(111) double-crystal system and higher harmonics was rejected with two mirrors. An energy of 25 keV was selected to avoid significant scattering at the Nafion membrane surface. All the measurements were performed at room temperature. Both the Pt thin film and the Pt(111) electrodes were exposed to the flow of air saturated with water vapor during the experiments. More detailed information is available in the Supporting Information.

## RESULTS AND DISCUSSION

Figure 2 shows an  $I$ – $V$  relation of the Pt thin film/PEM/PFSI/Pt(111) electrode. Potential was applied to the Pt(111) electrode with respect to the Pt thin film. Anodic current started to increase from about 0.6 V. Because the  $I$ – $V$  curve was measured in a two-electrode system, the electrode potential of each electrode, Pt thin film, and Pt(111) cannot be precisely determined. However, oxygen reduction and water oxidation should take place at the Pt thin film and Pt(111) electrodes, respectively, when anodic current flowed at the Pt(111) electrode because both electrodes are exposed to water vapor saturated air.

The (00) rod measurements were performed at the Pt(111) electrode, which is in contact with PFSI, without bias and at 1 V. Figure 3 shows the (00) rod profiles of the PFSI membrane/Pt(111) electrode interface measured (a) without bias and at (b) 1 V with respect to the Pt thin film. The interfacial structure normal to the surface was quantitatively determined from the least-squares fitting of the (00) rod data to a three-layer structure model on the Pt(111) surface with a kinematical calculation. Each layer was assumed to be consisting of Pt, C, O,  $\text{CF}_4$ ,  $\text{C}_2\text{F}_4$ , or  $\text{SO}_3^-$ .

The best fit data for the (00) rod profile of the Pt(111) surface measured without bias (Figure 3a) was obtained by assuming the Pt(111)-(1  $\times$  1) substrate/Pt(1)/Pt(2)/ $\text{C}_2\text{F}_4$  structure, as shown in Figure 4a. The coverage of the first Pt layer, Pt(1), and the second Pt layer, Pt(2), and the adsorbed  $\text{C}_2\text{F}_4$  layer are 1.00, 0.94, and 1.07 ML, respectively. The layer distances of the Pt(111)-(1  $\times$  1) substrate–Pt(1), Pt(1)–

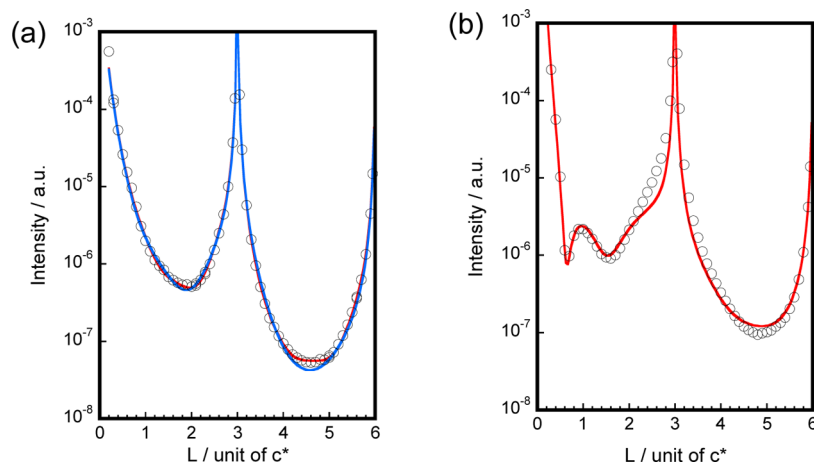


**Figure 3.** (00) rod profiles of the Pt(111) electrode measured (a) without bias and at (b) 1 V. Circles and solid lines are experimental data and calculated curves, respectively. Red solid lines represent fitted curves based on (a) Pt(111)-(1  $\times$  1)/Pt/Pt/ $\text{C}_2\text{F}_4$  and (b) Pt(111)-(1  $\times$  1)/Pt/Pt/O models. Blue solid line in (a) represents calculated curve based on the coadsorption model, Pt(111)-(1  $\times$  1)/Pt/ $\text{SO}_3^-$ – $\text{C}_2\text{F}_4$ .

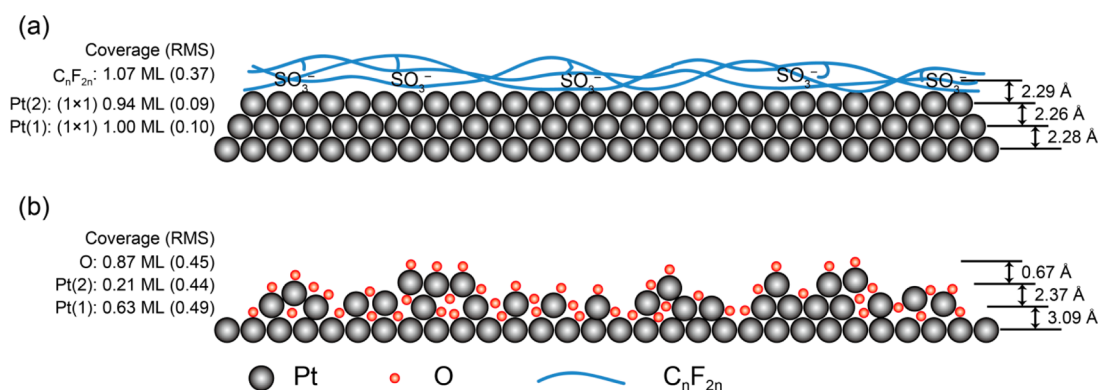


**Figure 4.** Schematic models based on structural parameters obtained from best fit data of Figure 3a,b.

Pt(2), and Pt(2)– $C_2F_4$  layers are 2.28, 2.26, and 2.29 Å, respectively. The layer distances between the Pt layers are in reasonable agreement with that calculated for the Pt layers with Pt atoms situated at the 3-fold hollow site on the Pt(111)– $(1 \times 1)$  surface, 2.27 Å. These results confirm that the ideal Pt(111)– $(1 \times 1)$  structure was formed by induction heating at 1600 °C under an argon/hydrogen stream, and the structure was maintained even after coating with PFSI film. The relatively small root-mean-square (RMS) factors support the formation of an atomically flat Pt(111)– $(1 \times 1)$  structure.

A few groups found a substantial interaction between sulfonate groups and the Pt electrode surface by a voltammetric approach<sup>25–28</sup> and infrared reflection absorption spectroscopy (IRRAS).<sup>27,29,30</sup> However, while the fitting for the Pt(111)– $(1 \times 1)$ /Pt/Pt/ $C_2F_4$  structure gave reasonable structural parameters, that for the Pt(111)– $(1 \times 1)$ /Pt/Pt/ $SO_3^-$  structure resulted in unreasonable parameters, suggesting that fluorocarbon chains of PFSI were present on the Pt(111)– $(1 \times 1)$  surface. One plausible model is the coadsorption of sulfonate groups and fluorocarbon groups, as shown in Figure 4a, where the adsorption of sulfonate groups can be hardly detected by SXS (have only a subtle effect on the (00) rod profile) because of the low coverage and high RMS. In fact, the simulated result based on the coadsorption of sulfonate groups and fluorocarbon groups, that is, the Pt(111)– $(1 \times 1)$ /Pt/ $SO_3^-$  &  $C_2F_4$  model, where 0.09 ML  $SO_3^-$  and 1.10 ML  $C_2F_4$  layers are adsorbed on the Pt(111)– $(1 \times 1)$  surface,<sup>31</sup> was not much different from the experimental result and the fitted curve based on the Pt(111)– $(1 \times 1)$ /Pt/Pt/ $C_2F_4$ . Thus, it was considered that sulfonate groups coadsorbed on the Pt(111) surface, although fluorocarbon groups were the major species.

The (00) rod profile obtained by keeping the bias at 1 V (Figure 3b) is totally different from that obtained without the bias application (Figure 3a), especially between  $L = 0.2$  and 2.9. The kinematic simulations show that this shape is typically observed when the apparent coverage of a few top layers was decreased.<sup>22</sup> The best fit data for the (00) rod profile of Pt(111) surface measured at 1.0 V (Figure 3b) was obtained by assuming the Pt(111)– $(1 \times 1)$  substrate/Pt(1)/Pt(2)/O structure, as shown in Figure 4b, among the simulations for various models with O,  $CF_4$ ,  $C_2F_4$ , or  $SO_3^-$  as an adsorbed layer on Pt or Pt oxide, although  $\chi^2$ , probability distribution in fitting, was somewhat higher than that of Figure 3a. The simulation shows that the coverage of the first Pt layer, Pt(1), the second Pt layer, Pt(2), and the O layer are 0.63, 0.21, and 0.87 ML, respectively. The interlayer distances of the Pt(111)– $(1 \times 1)$  substrate–Pt(1), Pt(1)–Pt(2), and Pt(2)–O layers are 3.09,

2.37, and 0.67 Å, respectively. The coverages of Pt(1) and Pt(2) layers are much less than 1, showing the penetration of O atoms into the Pt lattice because the presence of O atoms in the Pt lattice results in the lower apparent Pt coverage due to the fact that the electron density of the O atom is less than 10% of that of Pt. This result and the presence of the outermost O layer show the oxide formation, place exchange of oxygen, and the detachment of the adsorbed PFSI layer from the surface, as shown in Figure 4b. Relatively large interlayer distances and RMS factors for the Pt layers support the penetration of O atoms into the deeper layers by turnover between Pt and O atoms.

Detachment of the PFSI layer from Pt and Au electrode surfaces upon oxide formation was demonstrated by an electrochemical quartz crystal microbalance (EQCM) and electrochemical atomic force microscope (EC-AFM) in our separate experiments.<sup>24,32,33</sup> It is reasonable to consider that hydrophobic fluorocarbon chains desorbed from the surface upon the formation of Pt oxide, which is much more hydrophilic than Pt. In addition, the sulfate anion, which is analogous to the sulfonate group of PFSI, is known to desorb from the Pt surface when oxide was formed.<sup>34</sup> A recent neutron reflectometry study suggested the formation of a hydrophilic domain at the Nafion/Pt interface when Nafion was in contact with the Pt oxide surface.<sup>35</sup> Water molecules may penetrate between this hydrophilic domain and the Pt oxide surface.

## CONCLUSIONS

In conclusion, the structure of the PFSI/Pt(111) interface at the Pt thin film/PEM/PFSI/Pt(111) electrode junction, which is an approximation of the MEA configuration, and its bias-induced structural change were determined by utilizing the SXS technique. SXS measurement shows that fluorocarbon groups of PFSI adsorbed on the Pt(111)– $(1 \times 1)$  surface without bias. When a positive potential was applied to the Pt(111) electrode, Pt oxide was formed, the PFSI layer was detached from the Pt surface, and O atoms penetrated into the Pt lattice by turnover between Pt and O atoms. This work clarified the oxide formation process of the Pt electrode at an atomic level by using a well-defined Pt(111) surface incorporated in the MEA-like configuration.

## ASSOCIATED CONTENT

### Supporting Information

Experimental details and schematic illustrations of the spectroelectrochemical cell and Pt thin film/Nafion membrane/Pt(111) junction for in situ SXS measurement. This

material is available free of charge via the Internet at <http://pubs.acs.org>.

## AUTHOR INFORMATION

### Corresponding Author

\*E-mail: [uosaki.kohei@nims.go.jp](mailto:uosaki.kohei@nims.go.jp). Tel: +81-29-860-4301. Fax: +81-29-851-3362.

### Notes

The authors declare no competing financial interest.

## ACKNOWLEDGMENTS

The present work is partially supported by World Premier International Research Center (WPI) Initiative on Materials Nanoarchitectonics, and MEXT Program for Development of Environmental Technology using Nanotechnology from Ministry of Education, Culture, Sports, Science and Technology, Japan. The synchrotron radiation experiments were performed as projects approved by SPring-8 (proposal nos. 2008B1499, 2009A1532, and 2009B1307).

## REFERENCES

- (1) Kordesch, K. V.; Simader, G. R. *Chem. Rev.* **1995**, *95*, 191.
- (2) Winter, M.; Brodd, R. J. *Chem. Rev.* **2004**, *104*, 4245.
- (3) Borup, R.; Meyers, J.; Pivovar, B.; Kim, Y. S.; Mukundan, R.; Garland, N.; Myers, D.; Wilson, M.; Garzon, F.; Wood, D.; Zelenay, P.; More, K.; Stroh, K.; Zawodzinski, T.; Boncella, J.; McGrath, J. E.; Inaba, M.; Miyatake, K.; Hori, M.; Ota, K.; Ogumi, Z.; Miyata, S.; Nishikata, A.; Siroma, Z.; Uchimoto, Y.; Yasuda, K.; Kimijima, K. I.; Iwashita, N. *Chem. Rev.* **2007**, *107*, 3904.
- (4) Wagner, F. T.; Lakshmanan, B.; Mathias, M. F. *J. Phys. Chem. Lett.* **2010**, *1*, 2204.
- (5) Garsany, Y.; Epshteyn, A.; Purdy, A. P.; More, K. L.; Swider-Lyons, K. E. *J. Phys. Chem. Lett.* **2010**, *1*, 1977.
- (6) Koper, M. T. M., Ed. *FUEL CELL CATALYSIS: A Surface Science Approach*; John Wiley & Sons, Inc.: Hoboken, NJ, 2009.
- (7) Gasteiger, H. A.; Markovic, N. M.; Ross, P. N. *J. Phys. Chem.* **1995**, *99*, 8290.
- (8) Gasteiger, H. A.; Markovic, N. M.; Ross, P. N. *J. Phys. Chem.* **1995**, *99*, 16757.
- (9) Markovic, N. M.; Gasteiger, H. A.; Ross, P. N. *J. Phys. Chem.* **1995**, *99*, 3411.
- (10) Markovic, N. M.; Schmidt, T. J.; Stamenkovic, V.; Ross, P. N. *Fuel Cells* **2001**, *1*, 105.
- (11) Kolb, D. M. *Prog. Surf. Sci.* **1996**, *51*, 109.
- (12) Uosaki, K.; Ye, S.; Naohara, H.; Oda, Y.; Haba, T.; Kondo, T. *J. Phys. Chem. B* **1997**, *101*, 7566.
- (13) Naohara, H.; Ye, S.; Uosaki, K. *J. Phys. Chem. B* **1998**, *102*, 4366.
- (14) Wano, H.; Uosaki, K. *Langmuir* **2001**, *17*, 8224.
- (15) Honbo, H.; Sugawara, S.; Itaya, K. *Anal. Chem.* **1990**, *62*, 2424.
- (16) Magnussen, O. M.; Hagebock, J.; Hotlos, J.; Behm, R. *J. Faraday Discuss.* **1992**, 329.
- (17) Toney, M. F.; Melroy, O. R. Surface X-ray Scattering. In *Electrochemical Interfaces: Modern Techniques for In-Situ Interface Characterization*; Abruna, H. D., Ed.; VCH Publishers: New York, 1991; p 55.
- (18) Takahashi, M.; Hayashi, Y.; Mizuki, J.; Tamura, K.; Kondo, T.; Naohara, H.; Uosaki, K. *Surf. Sci.* **2000**, *461*, 213.
- (19) Wang, J. X.; Adzic, R. R. *J. Electroanal. Chem.* **1998**, *448*, 205.
- (20) Tamura, K.; Ocko, B. M.; Wang, J. X.; Adzic, R. R. *J. Phys. Chem. B* **2002**, *106*, 3896.
- (21) Kondo, T.; Morita, J.; Okamura, M.; Saito, T.; Uosaki, K. *J. Electroanal. Chem.* **2002**, *532*, 201.
- (22) Kondo, T.; Morita, J.; Hanaoka, K.; Takakusagi, S.; Tamura, K.; Takahashi, M.; Mizuki, J.; Uosaki, K. *J. Phys. Chem. C* **2007**, *111*, 13197.
- (23) Kondo, T.; Tamura, K.; Takakusagi, S.; Kitamura, K.; Takahashi, M.; Mizuki, J.; Uosaki, K. *J. Solid State Electrochem.* **2009**, *13*, 1141.
- (24) Sonsudin, F.; Masuda, T.; Ikeda, K.; Naohara, H.; Uosaki, K. *Chem. Lett.* **2010**, *39*, 286.
- (25) Subbaraman, R.; Strmcnik, D.; Paulikas, A. P.; Stamenkovic, V. R.; Markovic, N. M. *ChemPhysChem* **2010**, *11*, 2825.
- (26) Subbaraman, R.; Strmcnik, D.; Stamenkovic, V.; Markovic, N. M. *J. Phys. Chem. C* **2010**, *114*, 8414.
- (27) Gomez-Marín, A. M.; Berna, A.; Feliu, J. M. *J. Phys. Chem. C* **2010**, *114*, 20130.
- (28) Ahmed, M.; Morgan, D.; Attard, G. A.; Wright, E.; Thompsett, D.; Sharman, J. *J. Phys. Chem. C* **2011**, *115*, 17020.
- (29) Kendrick, I.; Kumari, D.; Yakaboski, A.; Dimakis, N.; Smotkin, E. S. *J. Am. Chem. Soc.* **2010**, *132*, 17611.
- (30) Ayato, Y.; Kunimatsu, K.; Osawa, M.; Okada, T. *J. Electrochem. Soc.* **2006**, *153*, A203.
- (31) In this simulation, where the  $\text{SO}_3^-$  and  $\text{C}_2\text{F}_4$  were coadsorbed on the  $\text{Pt}(111)-(1 \times 1)$ , that is, the  $\text{Pt}(111)-(1 \times 1)/\text{Pt}/\text{SO}_3^-/\text{C}_2\text{F}_4$  structure, the layer distances of the  $\text{Pt}-\text{C}_2\text{F}_4$  and  $\text{Pt}-\text{SO}_3^-$  were fixed to 2.29 Å, which is the layer distance of the  $\text{Pt}-\text{C}_2\text{F}_4$  obtained from the fitting based on the  $\text{Pt}(111)-(1 \times 1)/\text{Pt}/\text{C}_2\text{F}_4$  structure.
- (32) Masuda, T.; Ikeda, K.; Uosaki, K. *Langmuir* **2013**, *29*, 2420.
- (33) Masuda, T.; Sonsudin, F.; Singh, P.; Naohara, H.; Uosaki, K. Manuscript in preparation.
- (34) Wieckowski, A.; Kolics, A. *J. Phys. Chem. B* **2001**, *105*, 2588.
- (35) Wood, D. L.; Chlistunoff, J.; Majewski, J.; Borup, R. L. *J. Am. Chem. Soc.* **2009**, *131*, 18096.